Proc. SPIE, Vol.5631 (2005) p.134 ~ p.142 [9 pages]

Correction of photon statistics of quantum states in single photon detection

Gang Li, Tiancai Zhang , Yuan Li, and Junmin Wang
State Key Laboratory of Quantum Optics and Quantum Optics Devices,
Institute of Opto-Electronics, Shanxi University, Taiyuan, 030006, P.R.China

ABSTRACT

Single photon counting module (SPCM) has been widely used in quantum information processing (QIP) to investigate the novel quantum-mechanical phenomena. We analysis the effect of SPCMs on photon statistics of light fields by mean of Hanbury Brown and Twiss (HBT) configuration. It shows that the measured second-order degree of coherence $g^{(2)}$ and Mandel Q factor for different states are strongly corrected. The total efficiency and background are taken into account. The agreement between experiment based on the coherent as well as thermal fields and the theory is quite good.

Keywords: Single photon counting module (SPCM), Hanbury Brown and Twiss (HBT) experiment, second-order degree of coherence, Mandel factor.

ITRODUCTIONS

By the development of quantum information science, generation of quantum states, especially single photon state, plays an important role in implementation of quantum cryptography [1] and quantum computation based on the physical system of photons[2]. Recently, single atom laser[3] and deterministic single photon [4] were demonstrated. The most important criteria of characterizing the single photon state is the second-order degree of coherence $g^{(2)}$ and Mandel Q factor obtained by means of HBT experiment[3,5]. As the development of techniques, fast and high-efficiency single photon counting modules (SPCMs), with low dark counts, have been widely used in quantum information processing (QIP) to investigate the novel quantum-mechanical phenomena at the single-photon level. In this paper we analysis how such SPCMs affect the photon statistics based on the Hanbury Brown and Twiss (HBT) configuration. The overall quantum efficiency and the background are taken into account. The corrected second-order degree of coherence and the Mandel Q factor are obtained. We theoretically investigate several light fields, including coherent state, single photon Fock state, Fock state with photon number of 2, i.e., $|2\rangle$, single mode thermal state and squeezed vacuum state, and it shows that for different quantum states the corrections of measured $g^{(2)}$ and Mandel Q factors are different. We also experimentally measure the second-order degree of coherence $g^{(2)}$ of single mode thermal state and the coherent state, and the agreement between experiment and theory is quite good.

Quantum Optics and Applications in Computing and Communications II,
edited by G.-C. Guo, H.-K. Lo, M. Sasaki, S. Liu, Proc. of SPIE Vol. 5631
(SPIE, Bellingham, WA, 2005) · 0277-786X/05/$15 · doi: 10.1117/12.577925

MODEL OF DETECTION

The basic model is shown in Fig.1. $g^{(2)}$ and Q can be determined by well known HBT scheme which comprises two SPCMs (D_1 and D_2) and a 50/50 lossless beam splitter (BS). $|\psi\rangle$ is the input field which has intrinsic photon distribution $P_{in}(n)$. Suppose the overall detection efficiency, including the optical collection efficiency, propagation efficiency and the quantum efficiency of photon detectors, is η. This overall efficiency can be regarded equivalently as an attenuation of the incident field by an attenuator with intensity transmission of η and then the detectors have ideal quantum efficiency of unity. The second factor affecting the measured $g^{(2)}$ is the background, including the environment radiation and the dark counts of the SPCMs. The background can be taken as a weak coherent field $|\beta\rangle$, which has random Poissonian photon distribution $P(n) = \gamma^n \exp(-\gamma)/n!$ with $\gamma = |\beta|^2$ [5,6](see Fig.1).

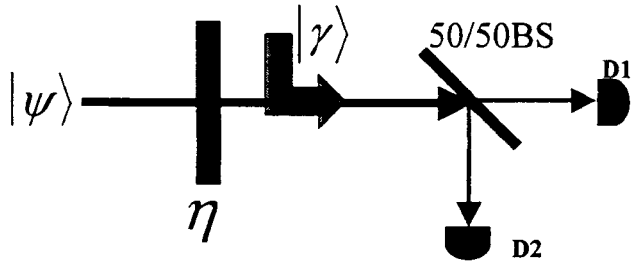

Fig. 1 Model of detection

The photon number distribution after the attenuator is [7]

$$P_{tr}(m) = \sum_{n=m}^{\infty} \frac{n!}{m!(n-m)!} \eta^m (1-\eta)^{(n-m)} P_{in}(n). \tag{1}$$

The beam is then mixed with the weak coherent background and the photon number distribution is given by [8]

$$P_{mix}(l) = \sum_{m=0}^{l} \frac{\gamma^{(l-m)}}{(l-m)!} \exp(-\gamma) P_{tr}(m). \tag{2}$$

The joint probability of detecting N photons on D_1 and (l-N) photons on D_2 can be written as [9]

$$P(N, l-N) = \frac{l!}{N!(l-N)!} P_{mix}(l). \tag{3}$$

Since each SPCM gives only one count within the dead time for one or more than one incident photons, there are totally four measured photon probabilities for the two detectors: $P(0,0)$, $P(0,1)$, $P(1,0)$and

$P(1,1)$. The coincident count probability P_{II} can be expressed as the sum of all the probabilities that each detector has one count:

$$P_{II} = P(1,1) = \sum_{l=2}^{\infty}\sum_{N=1}^{l-1}\left(\frac{1}{2}\right)^{l}\frac{l!}{N!(l-N)!}P_{mix}(l). \tag{4}$$

The probability of one count for D_1 or D_2 can be written as

$$P_{I} = P(0,1) + P(1,1) = \sum_{l=1}^{\infty}\sum_{N=0}^{l}\left(\frac{1}{2}\right)^{l}\frac{l!}{N!(l-N)!}P_{mix}(l). \tag{5}$$

And the measured mean photon number of the incident field according to the measured photon probabilities is $\langle n\rangle = 2P_I$. So the second-order degree of coherence can be obtained [7]

$$g^{(2)} = \left\langle :\hat{I}(t)\hat{I}(t):\right\rangle \Big/ \left\langle \hat{I}(t)\right\rangle^{2} = P_{II}/P_{I}^{2}, \tag{6}$$

where $\hat{I}(t)$ is the intensity of the fields in each port of the beam splitter, $\langle\ \rangle$ indicates ensemble average and :: denotes the normal ordering. The Mandel Q factor can be expressed accordingly as [10]

$$Q = \frac{\left\langle (\Delta n)^2\right\rangle - \langle n\rangle}{\langle n\rangle} = \frac{P_{II}(0)}{\langle n\rangle} - \langle n\rangle \tag{7}$$

NUMERICAL RESULTS

1. Coherent field

When the incident field is a coherent field with the intrinsic Poissonian photon distribution $P_{in} = \alpha^n \exp(-\alpha)/n!$, the above model gives the second order degree of coherence $g^{(2)}$=1 and Mandel factor Q=0, which are independent of the background and the detection efficiency.

2. Single photon state

If the input state is an ideal single photon state with P_1=1, thus we get the second order degree of coherence and Mandel parameter similarly. Fig.2 is the numerical results of $g^{(2)}$ and Q for single photon state. It shows in Fig.2 (a) that the measured $g^{(2)}$ for an ideal single photon source is strongly affected by the background and overall efficiency, on the contrary, in Fig.2 (b) the Mandel Q factor is not sensitive to the background. But in the case of zero background, $g^{(2)}$ keeps zero and is independent on the efficiency whereas for Mandel Q factor, it decreases linearly as overall efficiency increases, Q=-η.

The star in Fig.2 corresponds to the experimental data in reference [5]. In the experiment, the corresponding background is about γ=0.0022 and the overall efficiency is around η =4.55%, which gives the measured $g^{(2)}$=0.09 and Q=–0.04 for ideal single photon source. If the overall efficiency

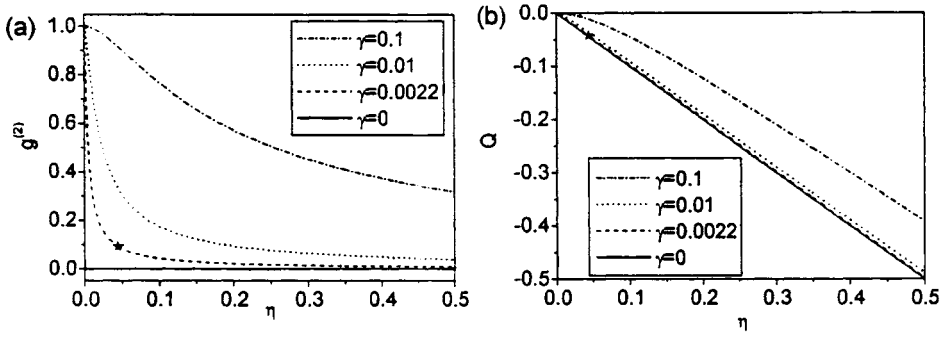

Fig. 2: The measured second-order degree of coherence $g^{(2)}$ (a) and Mandel Q factor (b) of single photon state as a function of overall efficiency η under different background: γ=0, 0.0022, 0.01 and 0.1. The star represents the experimental data in reference [5].

improves to 50%, the best quantum efficiency of present SPCM that we can get at 850nm, then the results can reach to $g^{(2)}$=0.009 and Q=–0.5 accordingly.

For the low overall efficiency, such as 5% in actual experiment [4,5], the Mandel Q factor is very close to zero. This Mandel Q factor cannot provide a distinct criterion to distinguish a single photon field from a coherent source, on the other hand, the second-order degree of coherence is more convenient to distinguish a single photon source when the overall efficiency can not be effectively improved but the background is relative low.

3. Fock state $|2\rangle$

If the incident field is a Fock state $|2\rangle$ which gives incident photon distribution P_2=1, using the above-mentioned procedures we get the detected $g^{(2)}$ and Q. Fig. 3 is the numerical results of the detected $g^{(2)}$ and Q as a function of detection efficiency. Compare to the single photon state the most interesting point is that even there is no background (solid line in Fig.3 (a)) the detected $g^{(2)}$ is larger than the theoretical value of 0.5 and reaches 0.89 for perfect detection, which is because that when both photons are incident on the same SPCM, the SPCM gives only one count. We can also see that for the Fock state $|2\rangle$ the detected $g^{(2)}$ and Q is always larger than that of single photon state while smaller than that of coherent state.

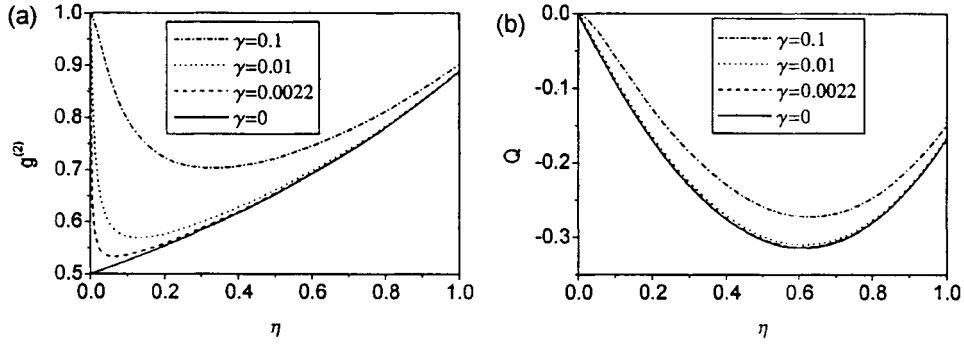

Fig. 3 The measured second-order degree of coherence $g^{(2)}$ (a) and Mandel Q factor (b) of Fock state $|2\rangle$ as a function of overall efficiency η under different background: γ=0, 0.0022, 0.01 and 0.1.

4. Thermal field

For a incident single mode thermal field, which has a Bose photon distribution $P_n = \frac{\alpha^n}{(1+\alpha)^n}$, the results are shown in Fig.4. We can see that when the background is diminished $g^{(2)}$ is close to the ideal value 2 at low η, and if η=1, $g^{(2)}$ reaches 1.5. As the background always exists, so $g^{(2)}$ is close to 1 when η is very low. But when η is becoming higher, $g^{(2)}$ will increase rapidly to a maximum and then drops slowly. For a certain η the second-order degree of coherence is smaller for a higher background.

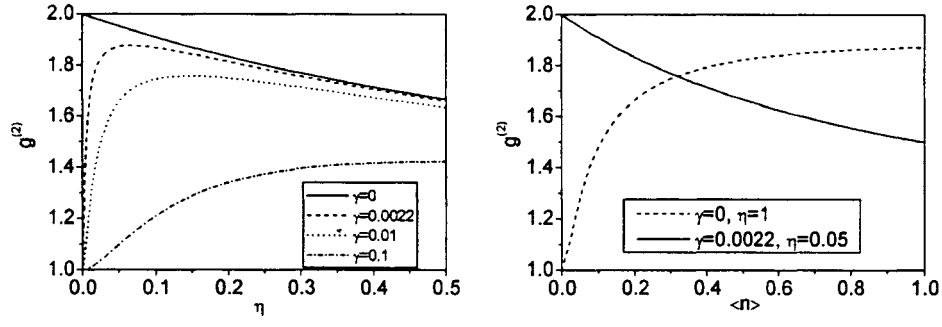

Fig.4 The measured second order degree of coherence $g^{(2)}$ as a function of total detection efficiency (a) and the detected mean photon number (b). In (a) we set the incident mean photon number of the thermal field is 1.

From Fig.4 (b) we can see that the measured $g^{(2)}$ depends the mean photon number even for perfect measurement, that is η=1 and γ=0, because of the correction of SPCMs themselves. It decreases from 2, the well-known result for a single-mode thermal state, when the mean photon number increases. For low mean photon number, $g^{(2)}$ is close to 2. At α=1 we get $g^{(2)}$ =1.5. But for real experimental situation, such as η=0.05 and γ=0.0022, the result is quite different. In this case, $g^{(2)}$ increases from 1 as the mean photon number increases from zero. Since for α=0, the detected field is only the Poissonian distributed background and consequently $g^{(2)}$=1. When α is becoming larger, $g^{(2)}$ is getting closer to 2.

5. Squeezed vacuum state (SVS)

The squeezed vacuum state has a photon distribution $P_{2n} = \frac{(\tanh r)^{2n}(2n)!}{\cosh r(n!2^n)^2}$ [11], where r is the squeezed factor. We can also get the measured $g^{(2)}$ as shown in Fig.5. The bunching effect is clearly obtained for SVS and the measured second-order degree of coherence $g^{(2)}$ is always higher than 2 and is becoming small when r is getting larger. $g^{(2)}$ is very sensitive to the efficiencies and backgrounds for lower squeezing, while for large squeezing it is not sensitive and the correction is very small. But in all these cases, the measured $g^{(2)}$ more or less reflects the real $g^{(2)}$ of the input SVS itself. This indicates that we can measure the squeezing of the SVS by measuring the $g^{(2)}$ on certain conditions when the correction is considered. Fig.5 (b) gives the change of $g^{(2)}$ as the detection efficiency varies, which is very similar to that of the single-mode thermal state.

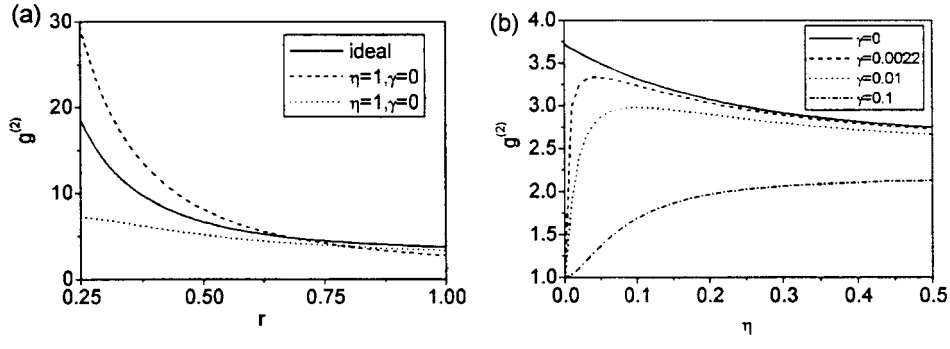

Fig.5 The detected second order degree of coherence $g^{(2)}$ as a function of detection efficiency (a) and the squeezed factor of the incident squeezed vacuum state (b). In (b) we set the squeezing factor r=1.

EXPERIMENT

We have done an experiment by using thermal field and coherent field to verify the model. The experimental setup is shown in Fig.6 (a). The thermal field is obtained by sending a coherent laser beam onto a rotating ground glass disk, and observing the random superposition of the diffracted contributions within a coherence time and a coherence area[12,13]. The coherent light is generated by a free-running grating-external-cavity diode laser with wavelength of 848 nm. The output light is focused by Lens1 with a 12.7mm focal length onto the ground glass disk driven by a small motor. The produced thermal field is a Gaussian field which has a coherent time related to the rotating speed of the ground glass disk[13]. The thermal light then hits onto a PBS (polarization beam splitter) with a $\lambda/2$ plate used to change the total efficiency of the system. After a pinhole the light is focused by Lens2 and split by a beam splitter (BS) and eventually received by D1 and D2 (SPCM-AQR-15, PerkinElmer), which have typical dead time about 40ns. The outputs of the SPCMs are fed into the data acquisition system. The band-pass filters used before the detectors have a transmission of 0.57, and the quantum efficiency of SPCM at 848nm is 0.5. So when the produced thermal field is completely transmitted through the PBS the overall detection efficiency of the system is 0.16. Background count rates of D1 and D2 are 0.95kHz and 1.19kHz, respectively. They are measured when the beam is blocked. This background count rate includes 40Hz of the dark count for each SPCM. The time resolution of the detection system is 32ns, which is used all the way in the experiment, and this gives the mean photon number of the background 6.9×10^{-5}.

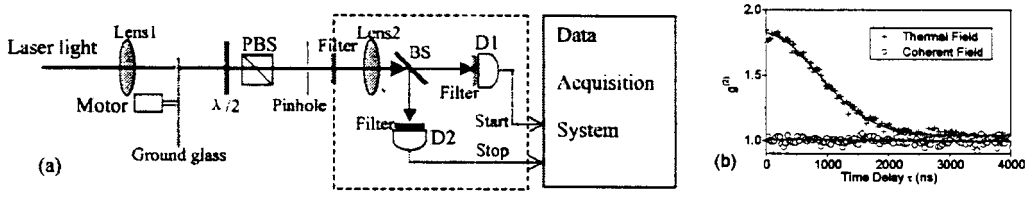

Fig.6 Setup of the experiment (a). Second-order degree of coherence of the thermal and coherent fields versus time delay of the two detectors (b). The count rates of D1 and D2 are 55.7kHz and 58.5kHz and the count rates of the background are 0.95kHz and 1.19kHz respectively. The number of starts is 10^6 and the sweep range is 128bins×32ns while time resolution (bin width) is 32ns.

The measured second-order degrees of coherence for coherent light and thermal light are shown in Fig.6 (b). The maximum count rates of D1 and D2 are 55.7kHz and 58.5kHz, respectively, which give the collected mean photon number of the thermal field 0.022. The output of D1 is set as start signal and output of D2 is set as stop signal, and we get the coincident counts of D1 and D2 on the time range of 4096ns (128bins×32ns). The solid line for thermal light is a Gaussian fitting. At zero time delay we get $g^{(2)}=1.83$, which is less than 2 and is reasonable as mentioned before. The coherent time of the thermal field is about 1.8μs in present status.

Rotating the $\lambda/2$ to change the overall detection efficiency, we get $g^{(2)}$ for different efficiencies, as shown in Fig.7 (a). The dashed line is the theoretical result when the produced field is an ideal thermal field and the measured mean photon number is $<n>=0.022$ with background $\gamma=0.000069$. The results give a relatively higher values of $g^{(2)}$ than the experimental data (square points in Fig.7 (a)). But if we consider the measured light is a mixture of 1% of coherent light and 99% of thermal light, that is, $\gamma=0.000068+0.01\times<n>\times\eta$, then we get the solid line in Fig.7 (a) and this agrees with the experimental results. The triangles in the figure are the experimental data for the coherent light and the dotted line is

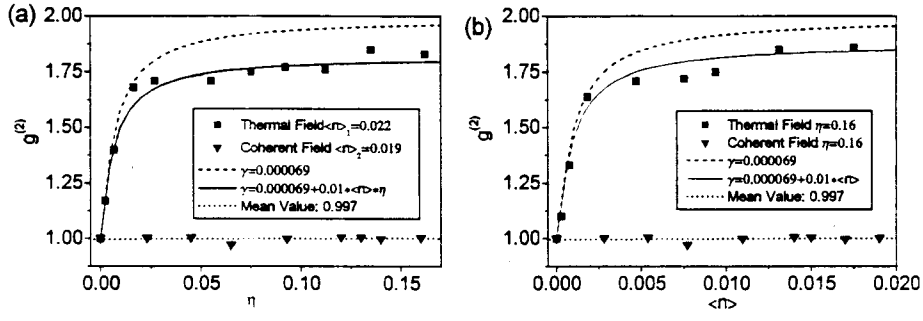

Fig.7 The second-order degree of coherence of the thermal and coherent fields versus the total efficiencies (a) and the mean photon number (b).

the mean value which leads to $g^{(2)}=1$, as expected.

When we change the intensity of the input light to vary the detected mean photon number, we get $g^{(2)}$ at different mean photon number. The results are shown in Fig.7 (b). The dashed line is the theoretical curve when the light is thought as a pure thermal field with a background $\gamma=0.000069$, similarly to above, the solid line corresponding to the case of 1% coherent light plus 99% thermal light. Again, agreement between experiment and theory is apparently quite good. The detected $g^{(2)}$ for coherent field (triangle points) is always around 1 which is not affected by the change of the input intensity.

ACKNOWLEDGMENT

The work is supported by the NSF of China under grant numbers (10434080, 10374062, 60178006), the TRAPOYT in High Education Institutions of MOE, and Research Funds for Youth from Shanxi Province(20031002). TCZ would like to thank Dr Liantuan Xiao for useful discussions.

REFERENCES

1. N. Gisin, G. Ribordy, W. Tittel, and H. Zbinden, Rev. Mod. Phys. 74, 145 (2002)
2. H.-J. Briegel, S. J. van Enk, J. I. Cirac, P. Zoller, in The Physics of Quantum Information, D. Bouwmeester, A. Ekert, A. Zeilinger, Eds.(Springer, Berlin, 2000)
3. J. McKeever, A. Baca, A. D. Boozer, J. R. Buck, and H. J. Kimble, Nature 425, 268 (2003)

4. J. McKeever, A. Baca, A. D. Boozer, R. Miller, J. R. Buck, A. Kuzmich and H. J. Kimble, Science 303,1992 (2004); Axel Kuhn, Markus Hennrich, and Gerhard Rempe, Phys. Rev. Lett., **89**, 067901 (2002)
5. F. Treussart, R. Alleaume, V. Le Floc'h, L. T. Xiao, J.-M. Courty, and J.-F. Roch, Phys. Rev. Lett. 89, 093601 (2002)
6. L. T. Xiao, Y. T. Zhao, T. Huang, J. M. Zhao, W. B. Yin, and S. T. Jia, Chin. Phys. Lett. 21, 489 (2004)
7. L. Mandel and E. Wolf, Optical Coherence and Quantum Optics, (Cambridge University Press, New York, 1995)
8. J. A. Abate, H. J. Kimble, and L. Mandel, Phys. Rev. A 14, 788 (1976)
9. R. A. Campos, B. E. A. Saleh, and M. C. Teich, Phys. Rev. A 40, 1371 (1989)
10. R. Short, and L. Mandel, Phys. Rev. Lett. **51**, 384 (1983)
11. H.-A. Bachor, *A Guide to Experiments in Quantum Optics*, (WILEY-VCH, 1998)
12. F. T. Arecchi, Phys. Rev. Lett. 15, 912 (1965)
13. L. Basano, and P. Ottonello, Am. J. Phys. 50, 996 (1982)